and C. L. Drake, Eds. (Springer-Verlag, New York, 1974), pp. 249–260.
16. J. C. Moore and D. E. Karig, *Geol. Soc. Am. Bull.* **87**, 1259 (1976).
17. L. D. Kulm and G. A. Fowler, in *Geology of Continental Margins*, C. A. Burk and C. L. Drake, Eds. (Springer-Verlag, New York 1974), pp. 261–283.
18. M. Langseth *et al.*, *Geotimes* **23**, 22 (1978).
19. R. von Huene *et al.*, *ibid.*, p. 16.
20. R. W. R. Rutland, *Nature (London)* **233**, 252 (1971).
21. S. Murauchi, *Kaiyo-Kagaku* **7**, 537 (1975).
22. M. G. Langseth, R. von Huene, N. Nasu, H. Okada, *Oceanologica*, in press.
23. S. E. Delong and P. J. Fox, in *Island Arcs, Deep Sea Trenches, and Back Arc Basins*, M. Talwani and W. Pitman, Eds. (American Geophysical Union, Washington, D.C., 1977), pp. 221–228.
24. T. Utsu, *J. Fac. Sci. Hokkaido Univ. Ser. 7* **3**, 379 (1971).
25. S. Murauchi and W. Ludwig, *Initi. Rep. Deep Sea Drill. Proj.* **56-57**, 463 (1980).
26. R. N. Anderson and M. D. Zoback, *ibid.*, in press.
27. A. B. Watts, J. K. Weissel, R. L. Larson, *Tectonophysics* **37**, 167, (1977).
28. T. Wantanabe, M. G. Langseth, R. N. Anderson, in *Island Arcs, Deep Sea Trenches and Back Arc Basins*, M. Talwani and W. Pitman, Eds. (American Geophysical Union, Washington, D.C., 1977), pp. 137–161.
29. M. E. Chapman and M. Talwani, *Geophys. J. R. Astron. Soc.*, in press.
30. C. G. Chase, *Nature (London)* **282**, 464 (1979).
31. M. Ewing and B. C. Heezen, *Science* **131**, 1677 (1960).
32. H. H. Hess, in *Petrologic Studies: A Volume in Honor of A. F. Buddington*, A. E. J. Engels *et al.*, Eds. (Geological Society of America, New York, 1962), p. 599.
33. F. J. Vine and D. H. Mathews, *Nature (London)* **199**, 947 (1963).
34. X. LePichon, *J. Geophys. Res.* **73**, 3661 (1968).
35. J. R. Cann, *Geophys. J. R. Astron. Soc.* **15**, 331 (1968).
36. M. G. Langseth, X. LePichon, M. Ewing, *J. Geophys. Res.* **71**, 5321 (1966).
37. J. B. Corliss *et al.*, *Science* **203**, 1073 (1979).
38. J. T. Wilson, *Nature (London)* **207**, 343 (1965).
39. B. C. Heezen, M. Tharp, M. Ewing, *Geol. Soc. Am. Spec. Pap. 65* (1959).
40. A. S. Laughton and R. C. Searle, in *Deep Sea Drilling in the Atlantic Ocean: Ocean Crust*, M. Talwani, C. G. Harrison, D. E. Hayes, Eds. (American Geophysical Union, Washington, D.C., 1979), pp. 15–32.
41. R. Hey, *Geol. Soc. Am. Bull.* **88**, 1404 (1977).
42. J. A. Orcutt, B. L. N. Kennett, L. M. Dorman, *Geophys. J. R. Astron. Soc.* **45**, 305 (1975).
43. A. W. H. Bunch and B. L. N. Kennett, *ibid.* **61**, 141 (1980).
44. R. E. Houtz, *Geol. Soc. Am. Bull.* **91** (Part 1), 406 (1980).
45. T. J. Herron, W. J. Ludwig, P. L. Stoffa, T. K. Kan, P. Buhl, *J. Geophys. Res.* **83**, 132, (1978).
46. T. J. Herron, P. Stoffa, P. Buhl, *Eos* **61**, 367, (1980).
47. F. M. Richter, *J. Geophys. Res.* **78**, 8735 (1973).
48. A. B. Watts, J. H. Bodine, N. M. Ribe, *Nature (London)* **283**, 532 (1980).
49. C. R. B. Lister, *Geophys. J. R. Astron. Soc.* **39**, 465 (1974).
50. R. N. Anderson, M. G. Langseth, J. G. Sclater, *J. Geophys. Res.* **82**, 3391 (1977).
51. J. M. Edmonds, *Eos* **61**, 129 (1980).
52. R. N. Anderson, M. A. Hobart, M. G. Langseth, *Science* **204**, 828 (1979).
53. CRRUST (Costa Rica Rift United Scientific Team), in preparation.
54. K. D. Klitgord and J. C. Behrendt, *Mem. Am. Assoc. Pet. Geol.* **29**, 85 (1979).
55. J. I. Ewing and M. Ewing, *Geol. Soc. Am. Bull.* **70**, 291 (1959).
56. R. E. Sheridan, J. A. Grow, J. C. Behrendt, K. C. Bayer, *Tectonophysics* **59**, 1 (1979).
57. P. L. Stoffa, P. Buhl, T. J. Herron, T. K. Kan, W. J. Ludwig, *Mar. Geol.* **35**, 83 (1980).
58. Lamont-Doherty Geological Observatory contribution No. 3168. This manuscript was reviewed by A. B. Watts, W. Pitman, and P. Rabinowitz. The GLORIA data from R. Searle in the SEABEAM map from V. Renard were kindly made available prior to publication. This work was supported by NSF grants DPP80-19461 and OCE 80-19452.

# Crustal Processes of the Mid-Ocean Ridge

East Pacific Rise Study Group

In 1854, Matthew Fontaine Maury published the first bathymetric chart of the North Atlantic Ocean, revealing the presence of a great ridge running down its central axis (*1*). Thought at that time to be a geosynclinal structure, the Mid-Ocean Ridge (MOR) has proved to be the largest single geological feature on the surface of the earth. Stretching for a distance of 72,000 kilometers and circling the globe, it covers over 28 percent of the planet's surface.

During the last quarter century, the MOR has assumed considerable importance in geological thought, particularly in the development of modern concepts of global tectonics. We now understand it as a site of mantle upwelling along which the lithospheric plates of the oceans develop. Until recently, the study of this great geologic province took place along several parallel but separate lines of inquiry, each focusing on different aspects of the ridge system: its surficial volcanism, heat budget, magnetic character, isostatic response, hydrothermal activity, crustal structure, suspected composition, and subbottom crustal processes. Within the last few years, however, these parallel studies have begun to converge on a central question: What is the nature of the magma chamber system that underlies the MOR and is thought to be responsible for the observed processes? What follows is a summary of these separate lines of evidence and a synthesis that attempts to present a unified model of the magma chamber system and its related crustal processes, the chemistry of the ocean itself, and the occurrence of massive sulfide deposits in the rifted central axis.

The members of the group (listed alphabetically) are as follows: Robert D. Ballard, Ocean Engineering Department, Woods Hole Oceanographic Institution, Woods Hole, Massachusetts 02543; Harmon Craig, Scripps Institution of Oceanography, La Jolla, California 92093; John Edmond, Department of Earth and Planetary Sciences, Massachusetts Institute of Technology, Cambridge 02139; Marco Einaudi, Department of Applied Earth Sciences, Stanford University, Stanford, California 94305; Robin Holcomb, U.S. Geological Survey, Vancouver, Washington 98663; Heinrich D. Holland, Department of Geological Sciences, Harvard University, Cambridge, Massachusetts 02138; Clifford A. Hopson and Bruce P. Luyendyk, Geology Department, University of California, Santa Barbara 93106; Kenneth Macdonald, Department of Geological Sciences, Marine Science Institute, University of California at Santa Barbara, Goleta 93106; Janet Morton, Geophysics Department, Stanford University; John Orcutt, Scripps Institution of Oceanography; and Norman Sleep, Geophysics Department, Stanford University.

## Gravity Structure and Seismology of the Mid-Ocean Ridge

A decade ago Dorman and Lewis suggested that the relationship between gravity and topography could be computed as a function of spatial wavelength (*2*). This technique was subsequently applied to investigations of ocean basins. Cochran (*3*) applied it to various segments of the MOR and concluded that (i) an elastic plate model which supports the topograpic load partly through flexural strength is required; and (ii) the plate thickness of the East Pacific Rise (EPR) is 2 to 6 km and that of the Mid-Atlantic Ridge (MAR) is substantially larger, 7 to 13 km. There are, however, some questions about whether on the basis of gravitational field data it may be possible to resolve this difference. In spite of these questions, the results are consistent with the idea that the lithospheric plates cool and thicken with time as they move laterally away from the spreading center.

Theoretical models of the temperature distribution near the ridge axis are in general agreement with the conclusions from gravity data. One can calculate the temperature in the region of the ridge axis by solving the vertical heat flow equation for steady-state emplacement and horizontal displacement away from


0036-8075/81/0703-0031$02.00/0  

*Summary.* Independent geological and geophysical investigations of the Mid-Ocean Ridge system have begun to focus on the nature of the magma chamber system underlying its central axis. Thermal models predict the existence of a steady-state chamber beneath a thin crustal lid ranging in thickness from 2 to 13 kilometers. The only aspect of the system that these models fail to account for is the extremely slow spreading rates. Seismological studies reveal the existence of a low-velocity zone beneath segments of the East Pacific Rise, which is thought to correspond to a chamber system having a half-width of approximately 5 to 10 kilometers. These estimates compare favorably with those derived separately through petrological investigations of deep-sea drilling results, various sampling programs, and field and laboratory studies of ophiolites. The chamber is thought to be wing-shaped and to remain continuously open; it is thought to be fed from the center while simultaneously solidifying at the sides as spreading carries the two halves apart. Progressive fractionation occurs by crystal settling coupled with repeated replenishment and magma mixing in an open steady-state system. Near-bottom studies reveal that the zone of extrusion above the chamber is narrow, but its eruptive history is cyclic in nature, in conflict with the predictions of a steady-state model. On-bottom gravity data at 21°N on the East Pacific Rise reveal a negative gravity anomaly that may be related to the uppermost part of the chamber. The anomaly is only 2 kilometers wide and 1 kilometer below the sea floor. This feature may be associated with a short-term upper magma reservoir. The cyclic volcanic activity is directly related to the active phase of hydrothermal circulation responsible for the observed negative thermal anomaly. The volume of water associated with this circulation is equal to the entire ocean volume passing through the accretion zone approximately every 8 million years. This is about 0.5 percent of the world's rivers, but the effective transport rates of elements are comparable to those of rivers in that anomalies for individual elements are frequently between 100 and 1000 times the average river composition. The degree of subsurface dilution determines the final exit temperature and composition of the hydrothermal fluids, ranging from manganese domination at extreme dilution to iron at intermediate levels to sulfide deposition when low dilution occurs. The discovery of massive sulfide deposits on the East Pacific Rise is destined to have a profound impact on our understanding of ore-forming processes. Whether it will have any economic significance remains to be seen.

the ridge axis, using energy-conserving boundary conditions (*4, 5*). It is found from these calculations that the lateral conduction of heat causes a cool lid of crust to exist at the ridge axis. A steady-state magma chamber may exist in the hot crust beneath this lid close to the plate boundaries. The thickness of the lid is inversely proportional to the spreading rate beyond a minimum thickness of 2 km or so because of hydrothermal cooling. For intermediate spreading rates (6 centimeters per year), a lid at least one additional kilometer thick is required.

Marine seismologists have also produced several independent arguments supporting the existence of a localized shallow magma chamber beneath the EPR (Fig. 1). Experiments beginning in 1975 have revealed at several places on the EPR a low-velocity zone interpreted as representing a magma chamber (*6–8*). A second series of experiments, which obtained profiles on mature oceanic crust, revealed a seismic stratigraphy consistent with rock types encountered in various ophiolite suites (*9, 10*).

Evidence for the existence of a crustal low-velocity zone on the ridge crest, potentially corresponding to a magma chamber, was first published in 1975 (*6*) for the EPR at 8°N. This work was coincidental with theoretical work which broke substantially with earlier approaches to treating explosion data. In the older studies, models consisting of thick homogeneous layers were constructed to fit the travel time data (*11*). With the new techniques it was possible for the vertical variation to be quite arbitrary, and, even more important, the resultant errors could be quantitatively estimated (*12*). In addition, the application of synthetic seismograms to the analysis of seismic profiles begun by Helmberger (*13*) was developed to the point that accurate and complete synthetic seismograms could be inexpensively computed in complicated attenuative media containing low-velocity zones (*14*). The primary evidence for the existence of a low-velocity zone was the presence of a broad shadow zone beginning at ranges of approximately 15 km where the wave amplitudes, consisting largely of diffracted and tunneled energy, dropped off dramatically and the travel times were substantially delayed (*7, 15*). Research at 8°N on the EPR (with a total opening rate of 12 cm/year) based on sonobuoy refraction data (*8*) and near-vertical reflection profiling (*16*) further supported the existence of a shallow seismic shadow zone. In a similar fashion, Reid *et al.* (*15*) reported evidence suggesting the occurrence of a shallow magma chamber at 21°N (6 cm/year). Additional support for the attenuative nature of the crustal structure of the rise in this general area was provided by the anomalous damping of high-frequency shear waves propagating along the axis; this finding suggested the presence of a shallow chamber less than 10 km wide (*17*).

Rosendahl *et al.* (*18*), Bibee (*19*), Russell (*20*), Mueller (*21*), and Scarlett (*22*) reported the presence of pronounced low-velocity zones beneath the EPR at 10°S (16 cm/year) and the Galápagos Rift at 86°W (6 cm/year). Although Bibee and Rosendahl *et al.* disagree on the depth of the magma chamber, the appearance of the shadow zones at 12 to 15 km argues that the overlying lid must be thin.

The width, as well as the vertical extent and position of the chamber, are also important. On the basis of sonobuoy lines parallel to the ridge, Rosendahl *et al.* (*8*) demonstrated that the width is at least 10 km. This value is consistent with that estimated by McClain and Lewis (*17*) and Reid *et al.* (*15*), although the width may be even greater as the chamber pinches out in both directions of plate motion.

## Petrological Constraints on the Magma Chamber

Petrological studies within the last few years have also produced strong independent evidence for a shallow magma chamber, the character of oceanic crust formed beneath the ridge being controlled by the differentiation and mixing of mantle-derived magma in a steady-state chamber near the surface. The evidence comes from fresh MOR basalts and glasses obtained from submersible studies, from the Deep Sea Drilling Project (DSDP) and dredging studies, and from field and laboratory studies of ophiolites. Well-preserved ophiolites provide exposed cross sections of former oceanic crust and upper mantle (Fig. 2a). The stratigraphic thickness of the volcanic and sheeted dike zones, which lie above the plutonic part of the ophiolite, gives the depth to the top of the magma chamber, and the transition from plutonic (chiefly gabbroic) igneous rocks to underlying peridotite tectonites shows

details of the Mohorovicic seismic discontinuity (*23, 24*). The plutonic sequence itself offers a direct view of the former magma chamber, revealing its vertical dimension and the stratigraphy, structure, and compositional variation of its differentiation products. Cumulates generally comprise the major part of the plutonic section. Here the cumulus sequence, especially its cryptic and cumulus-phase variation, reveal in detail how the fractionating magma evolved along the crystal line of descent. The overlying volcanic rocks and sheeted dikes represent the complementary melts (plus their intratelluric crystals) which fractionated along the liquid line of descent.

Petrologic and geochemical studies of fresh basaltic glasses and coexisting crystals in young unaltered lavas collected from modern oceanic spreading centers provide the best information on the compositional variation of the derivative melts tapped from the magma chamber. This compositional variation reveals how the differentiated magma evolved along the liquid line of descent and how fractionation has been retarded by replenishment and magma mixing (*25*). The compositional variation of young lavas along the central rift axis of spreading ridges, mapped in submersible studies and acoustically positioned dredging, reveals how the composition of the underlying magma varies spatially (*26, 27*), whereas the compositional variation of eruptive sequences at a single site, obtained from submersible studies and deep-sea drilling, shows how the fractionating magma varies with time (*28*). The range of compositional variation is a measure of the extent to which magma has fractionated beneath the site of eruption, and it is significant that the fractionation range of these lavas does not begin to approach that of the underlying plutonic sequence, displayed in ophiolites.

Petrologic constraints on the size and shape of the magma chamber come chiefly from the igneous stratigraphy of ophiolites. Igneous cumulates that lie above peridotite tectonite are clearly crystallizing phases that have built up from the floor of the chamber by gravitational settling (Fig. 2a). The cumulates grade up into nonlayered isotropic gabbros formed by the simultaneous settling of crystals in clouds so dense that layering and planar lamination were no longer possible; gravitational differentiation within this zone is like that within the lower half or two-thirds of thick differentiated diabase sills on land (*29*). These isotropic "quasi-cumulates" grade upward into quartz-bearing hornblende gabbros, diorites, and small bodies of

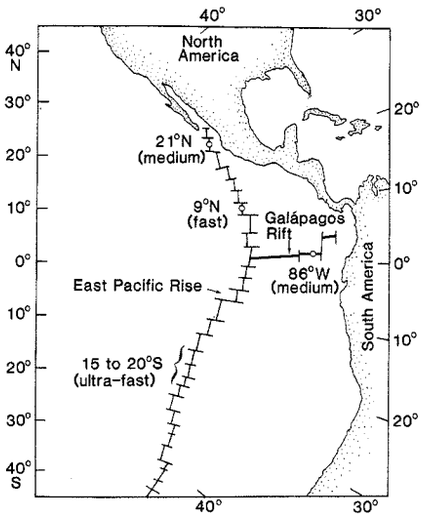


Fig. 1. Location of the East Pacific Rise and Galápagos Rift.

plagiogranite—an assemblage representing the most fractionated rocks of the entire ophiolite suite (Fig. 2a). These rocks grade back up into an uppermost zone of less fractioned gabbro and diabasic gabbro that have intrusive contacts against the overlying sheeted dikes but that are themselves cut by late-stage dikes and small plagiogranite intrusions which rise from the underlying fractionated zone (Fig. 2a). This uppermost zone of isotropic gabbros has crystallized downward from the roof of the magma chamber, which is represented by the sheeted dike zone; these are the "plated gabbros" of Dewey and Kidd (*30*). Thus, during solidification of the magma chamber, isotropic gabbros crystallized ("plated") downward from the roof while ultramafic and gabbroic cumulates and isotropic gabbro "quasi-cumulates" accumulated progressively upward from the floor. The parts of the magma chamber solidifying downward and upward meet in a "sandwich zone" where the progressively fractionating magma reached its most evolved composition. The quartz-bearing gabbros, diorites, and minor plagiogranites are included in this sandwich zone.

Spudich and Orcutt (*9*) have examined a suite of seismic refraction profiles with very-high-quality shear waves to derive models of $V_p/V_s$ or Poisson's ratio (the ratio of the fractional transverse contraction to the fractional longitudinal extension of a body under tensile stress) versus depth. These models have been compared with the physical properties of ophiolite suites (*31*) to reveal a pattern identical to the observed ophiolite stratigraphy. That is, the "oceanic layer" is clearly formed in a basalt differentiation sequence. Quite surprisingly, Poisson's ratio in a depth range of 1.5 to 2.5 km drops to less than 0.24, indicating the possible presence of substantial quartz. This observation is consistent with the presence of late-stage differentiates such as plagiogranite and quartz-bearing diorite in the sandwich zone. The presence of these diorites and plagiogranites may also provide a realistic model for the high magnetization necessary to make the oceanic layer a viable source for much of the amplitude of the observed marine magnetic anomalies.

The stratigraphic position of the sandwich zone (Fig. 2a) is the critical factor that determines the cross-sectional shape of the magma chamber (Fig. 2b) (*32*). This assumes a sea-floor spreading model in which the chamber remains open in the center and the two halves spread apart, as solidification ("plating") downward from the roof and accumulation upward from the base take place. The sandwich horizon marks the level at which the last most fractionated portion of magma was entrapped at the far side of each chamber half. The sandwich zone invariably occurs at high stratigraphic levels in ophiolite plutonic sequences that are reasonably well preserved and well studied petrologically (*24, 32–35*). In other words, each half-chamber solidified mainly by the accumulation of settled crystals upward from

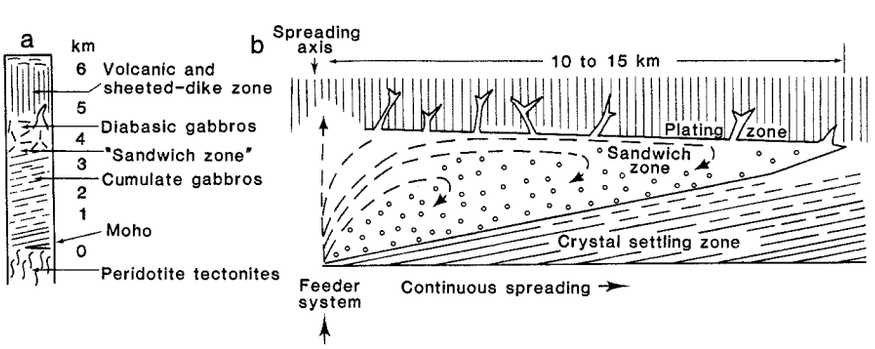


Fig. 2. Schematic model for a steady-state, continuously opening magma chamber (b) beneath a moderate- to fast-spreading ocean ridge. The model applies specifically to the Somali ophiolite gabbroic section in (a).

the floor, with only minor plating downward, as sea-floor spreading carried the two halves apart. This process results in a magma chamber with a nearly triangular or funnel-shaped cross section that widens upward (*32, 33, 36*). Models of spreading-axis magma chambers that widen downward (*26, 30, 37*) imply more downward plating than upward accumulation, which would result in a very thick noncumulus upper section and a sandwich zone located at a relatively low stratigraphic level within the plutonic sequence. We know of no well-documented examples of an ophiolite sequence with this kind of stratigraphy. Therefore, a magma chamber model with the general features of Fig. 2b (*32, 36*) is tentatively adopted as a working hypothesis for moderate- to fast-spreading ridge segments of the MOR.

The width of the magma chamber depends on its vertical height at the spreading axis and on the surface slope of the pile of cumulates that build up on each side. Plutonic sequences up to 5 or 6 km thick are known for some ophiolite complexes (*32, 36, 38*), and this may approach the upper limit for the vertical dimension of magma chambers at fast-spreading ridges. The slope angle at which cumulates will stand without slumping extensively is less easily estimated but may exceed that of wet sediments, because the adcumulus crystallization mechanism that accompanied the solidification of most of these layers would give added cohesion (*32, 36*). A cumulus slope angle of approximately 20° has been estimated for part of the Somali ophiolite (Oman), from the vergence angle of gabbroic cumulates onto the peridotite floor. Pallister and Hopson (*36*) estimate that the half-width of the Somali ophiolite magma chamber (Ibra section) is on the order of 10 to 15 km; their estimate is based on a 20° slope angle and a 5-km thickness for the cumulus sequence at this point. The seismic data of Rosendahl *et al.* (*18*) and Bibee (*19*) support a model with this type of geometry.

A comparison of the compositional variation of ocean-ridge lavas with that of plutonic sequences in ophiolites shows that the spectrum of ocean-ridge lavas is rather restricted [the silicon dioxide ($SiO_2$) range is chiefly within 48.5 to 52 percent, and the ratio of ferrous oxide to magnesium oxide ($FeO^t/MgO$) is about 0.7 to 1.9, rarely 3.2], whereas rocks that evolved along the liquid line of descent in the magma chamber, seen in the upper noncumulus parts of ophiolite plutonic sections, exhibit a broad spectrum from olivine gabbro and diabase through magnetite-rich diorite ($FeO^t/MgO = 4$) to plagiogranite ($SiO_2$ up to 76 percent) (*24, 39, 40*). A likely explanation for why a full range of differentiated magma compositions develops within the chamber while the magma extruded as lava within the rift valley has a much more limited compositional range is that fractionation within the magma chamber produces highly evolved intermediate to siliceous residual melts only after spreading has carried away the chamber halves well beyond the main zone of rifting and extrusion. In Fig. 2b extreme fractionation occurs only far out in the wings of the steady-state chamber (*32, 36*). In contrast, models in which the entire width of the magma chamber lies beneath the zone of extrusion (*26, 41*) do not satisfactorily account for the great compositional difference between the intrusive and extrusive suites.

A question then arises whether such magma chambers exist at all beneath the slow-spreading ridges (*42*). Below spreading rates of about 2 cm/year, lateral heat conduction might prevent a steady-state crustal magma chamber from existing (*4*). The greater thicknesses (7 to 13 km) predicted for the plate at the axis of the MAR (*5*), the failure of seismic experiments to detect broad crustal low-velocity zones, and the reported substantial depths of earthquakes (approximately 8 km) within the axial valley (*43*) argue for substantial differences between magma body geometries for slow- and fast-spreading systems.

Critical evidence for the existence of magma chambers also comes from the compositional variation of basaltic glasses (melts) from ocean-ridge lavas and the composition of their coexisting olivines. Melts coming directly from the upper oceanic mantle have primitive compositions, estimated by some workers to be tholeiitic picrite (*44*) and by others to correspond to the least fractionated tholeiitic MOR basalt recovered from the oceans (*45*). These melts have liquidus olivine of composition 90 to 91 mole percent forsterite, in equilibrium with the olivine of upper-mantle peridotite, and they deposit a basal zone of cumulus dunite with olivine (90 mole percent forsterite) where they first enter the magma chamber, as revealed in ophiolites (*36, 40, 46*). Ocean-ridge lavas having these and other primitive geochemical characteristics (*47*) are scarce. The spectrum of basaltic glass compositions from the vast majority of ocean-ridge lavas are fractionated to varying degrees (*48*), and coexisting olivine is typically in the range 75 to 85 mole percent forsterite. Least-squares mixing calculations show that these fractionated melts are derived from the melts of more primitive composition by removal of varying proportions of olivine, plagioclase, and clinopyroxene, the phases that crystallize early from MOR magmas at low pressures (*26, 49*). These are also the most common cumulus phases in ophiolite plutonic sequences, regarded as fossil magma chambers. Thus, most of the magma erupted as lava along the spreading ocean ridges appears not to have come straight from the mantle but to have fractionated in shallow crustal reservoirs en route to the surface.

Much progress has recently been made in understanding the processes that take place within the axial magma chambers and the control they exert on the composition and structure of the oceanic crust. Especially important is the accumulating evidence that these magma chambers fractionate as open systems, dominated by repeated replenishment and magma mixing. The evidence for magma mixing seen in the lavas includes phenocryst compositions and melt inclusions that are not in equilibrium with their enclosing melt (glass) and also chemical data which show that lava suites lie along straight-line mixing trends between more primitive and more evolved compositions rather than along the curved fractionation trends (*28*). In ophiolite cumulus sequences a cyclic pattern of cumulus phases reflects replenishment of melts that were fractionating down the olivine-plagioclase-clinopyroxene cotectic by repeated addition of more primitive melts that lay in the olivine liquidus field (*32, 34, 36*). The cryptic variation pattern shows that the magma composition alternated from progressive fractionation trends leading toward more evolved compositions to mixing trends that moved the melt back toward more primitive compositions (*36, 46*). The sum of evidence from the volcanic and plutonic rocks for progressive fractionating by crystal settling, coupled with repeated replenishment and magma mixing, harmonizes with the concept of an open-system, steady-state magma chamber that remains continuously open and is fed from the center while simultaneously solidifying at the sides as spreading carries the two halves apart.

An on-bottom gravity survey across the EPR crest at 21°N (Fig. 3) (*50*) revealed a negative gravity anomaly of about 1.5 milligals, which may be related to a crustal magma chamber. However, the fact that the anomaly is only about 2 km wide suggests that it may be due to the shape of the topmost part of the

chamber closest to the axis rather than to the entire wedge structure. If the anomaly is modeled as due to a horizontal cylinder, then the body could have a negative density contrast of 0.21 gram per cubic centimeter and a diameter of 750 meters with its center about 1 km below the sea floor. The gravity anomaly mapped over the EPR at 21°N indicates a total mass deficiency of $9 \times 10^7$ kilograms per meter of ridge length (*50*). If this deficiency is due to the top edge of a magma chamber, it could be isostatically balanced locally by 50 to 60 m of uplift of a topographic block 1 km wide at the crest. It can be argued that tectonic zone 1 (Fig. 3) is somewhat elevated above its surroundings, by about 20 to 30 m. However, it does not appear clear that the residual anomaly at the crest is completely compensated at this location by topography. Either friction or fault planes are maintaining disequilibrium, or compensation is by a broader scale process.

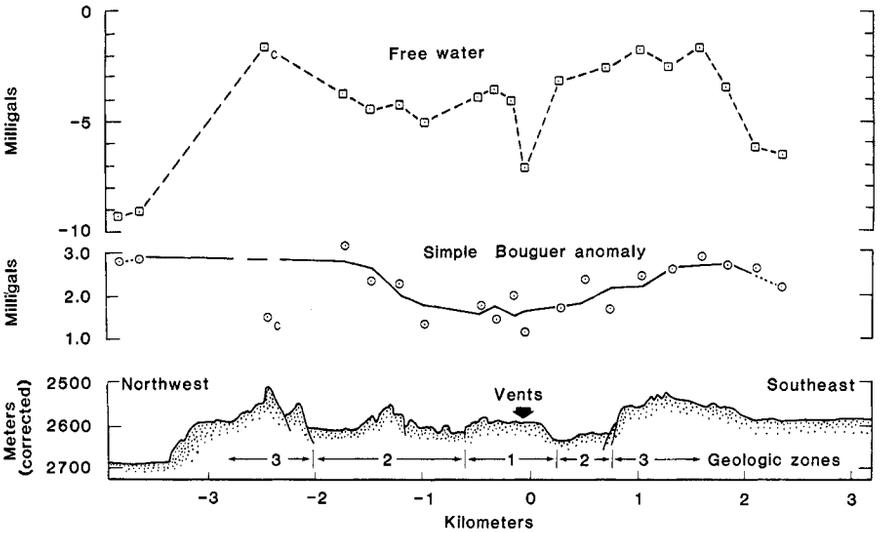


Fig. 3. A bathymetric profile across the EPR crest at 21°N taken with deep tow along with the simple Bouguer anomaly and free water anomaly measured at on-bottom gravity stations. The solid line is a three-point running mean, excepting the station at −2.4 km. The very low value at −2.4 km is due to the topographic effect of a hill which has been only partially corrected. The broad negative value centered about 0 km may be due to a shallow magma chamber (*50*).

The composition of ocean-ridge magmas is determined by (i) partial melting processes at one or more mantle sources, (ii) crystal fractionation and reaction of the melt with enclosing peridotite as it rises through (or with) upwelling upper mantle, (iii) crystal fractionation in shallow magma chambers, combined with (iv) replenishment and magma mixing, and (v) possible further modification of the derivative melt as it rises from the magma chamber to the surface.

Geochemical studies of the minor elements of basalts from the slow-spreading MAR have led some workers to conclude that magma batches with differences determined in the mantle can still be recognized in the lavas, even those from single DSDP drill holes (*51*) or from local areas within the rift valley (*52*). Very small or transitory magma chambers are implied, if processes (iii), (iv), and (v) are insufficient to erase the magma chemistry inherited from the mantle. Chemical and petrologic characteristics attributed to mantle processes should lessen and disappear, however, in lavas at progressively faster spreading ridges, where mantle melts would be more extensively mixed and homogenized in a larger magma chamber. If these characteristics remain, however, one would look to shallow crustal processes (v) as an alternative to mantle explanations. In this regard, little attention has as yet been paid to the possibility that magma rising to the surface from ridge-axis magma chambers might move haltingly and be temporarily stored in dike systems, where it could come in contact and interact with hot hydrothermal fluids circulating through the highly fissured upper crust. Such interactions would doubtless not change the major element chemistry of the melt, but they could have a significant effect on the minor elements. Phrased differently, can small volumes of magma pass through fissure systems in crust undergoing active hydrothermal metamorphism and emerge without any chemical imprint of that process?

## Volcanism, Structure, and Magnetics of the Rift Valley

Detailed studies of the surficial geology of the rift valley in the MAR and EPR reveal that the spreading processes are highly variable through time and space along the narrow rift (Fig. 4). The zone of active extrusive volcanism is generally less than 1 to 2 km in width and is flanked by a zone of extension dominated by faulted blocks.

The narrowness of the extrusive zone is also reflected in the nature of magnetic reversal boundaries. The sharpness of the magnetic polarity transition provides a measure of the width of formation for the upper oceanic crust (*53*). The sharpness of the magnetic transition imposes an upper limit for the width of formation of 1 to 5 km for the EPR (*54, 55*). Macdonald *et al.* (*55*) conducted a three-dimensional Fourier inversion treatment of deep-towed magnetic data over the Bruhnes-Matuyama reversal boundary on the EPR at 21°N. The reversal boundary in map view is remarkably linear, and the transition is only 1.0 to 1.4 km wide, an indication that the zone of crustal emplacement is only 0.6 to 1.0 km wide. Magnetic gradiometer measurements obtained by submersibles show that the reversal boundary in the exposed pillows and sheet flows occur 500 m farther away from the axis than the reversal boundary located by the inverted potential-field measurements. This 500-m overlap is an indirect measure of the "spillover" of volcanic flows away from the central axis at the same time that the crust is formed. In this area lava flows were observed to extend 500 m past the integrated transition (*56*), but in other areas of the EPR sheet flows appear to have traveled several kilometers off-axis (*57*) while in segments of the Galápagos Rift the young lava flows occupy the entire 4-km width of the rift valley (Fig. 4) (*58*). Even more remarkable than the sharpness of the polarity transition is the uniformity of polarities found on either side of the boundary. Even on long traverses (total of 4 km) to either side of the polarity boundary, every magnetic target had the correct polarity, that is, a polarity that agreed with the underlying regional magnetic stripe. This is not too surprising for the young side of the reversal boundary, since newer polarity crust should overlie the older. However, it is quite surprising that there were no outliers of new (+) polarity crust on the older (−) side of the boundary. The boundary is actually exposed along some of its length as a geologic contact between positive volcanic flows butting up against axially dipping fault scarps and as positive sheet flows lapping up to negative pillow flows.

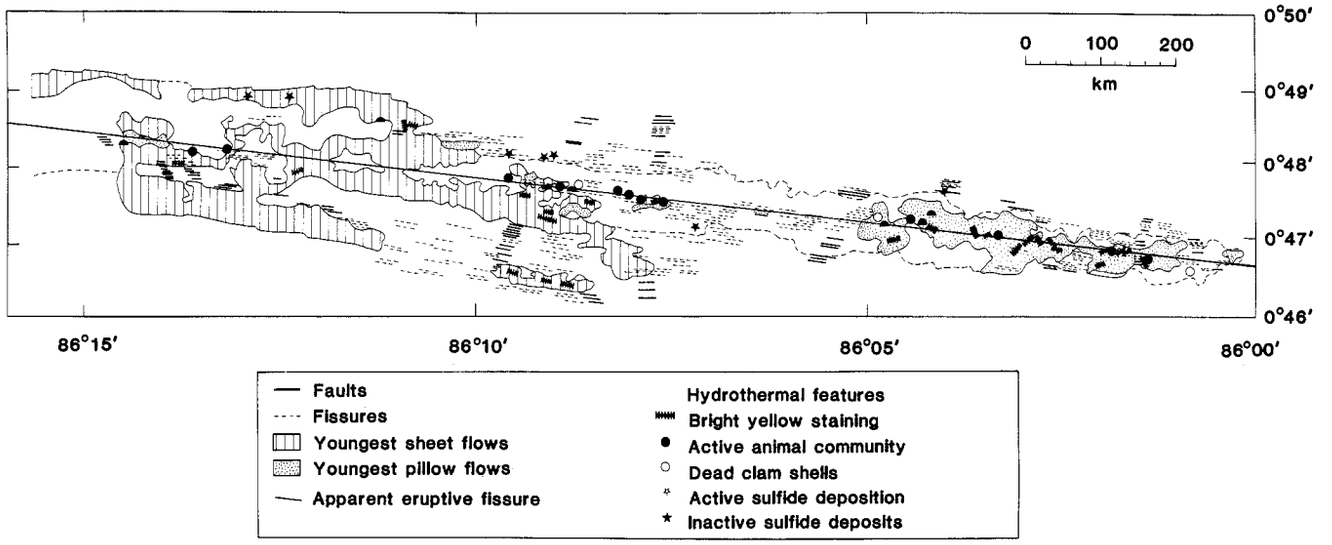


Fig. 4. Simplified geologic map of the Galápagos Rift showing the variation in the cyclic volcanic pattern along strike, as well as the location of active hydrothermal vents within the narrow zone of most recent extrusive volcanism (*98*).

How can this extraordinarily neat picture be reconciled with the complex magnetic stratigraphy found in deep-sea drilling holes? Holes that penetrate deeper than 500 m occur in the Atlantic, characterized by slow spreading rates. Statistical studies (*59*) show that at such slow rates a zone of crustal formation wider than a few kilometers will generate a crustal section with a potpourri of magnetic polarities. At faster rates with a narrow zone of crustal formation (EPR), boundaries will slope because of the overlap of newer polarity crust onto older, but the stripes will have a greater tendency toward magnetic homogeneity and magnetic anomalies will be sharper. Thus the formation of magnetic anomalies may be profoundly influenced by spreading rate and plate boundary width.

The nature of the volcanic activity can be inferred from analogies with subaerial landforms (*57*). Various morphologic flow types have been observed, and they are classified in two main groups, pillow lavas (*60*) and sheet flows (*57*). These types appear to be analogous to two kinds of subaerial pahoehoe, tube-fed (*61*) and surface-fed (*62*), respectively. Like their subaerial counterparts, pillow lavas and sheet flows seem to arise from differences in the duration of the flow, which, in turn, reflect variation in the behavior of eruptions and processes within the magma chamber. It is therefore possible to use lava-flow morphology to infer the character of the eruptions. By analogy with subaerial basalts, the sheet flows characterize brief eruptions with comparatively high effusion rates whereas pillow lavas tend to result from sustained eruptions with lower effusion rates. Eruption sequences along a subaerial rift zone commonly begin with brief eruptions that are dispersed in time and space and are followed by sustained eruptions from restricted localities along the rift zone. The net result of such a sequence is a complex assemblage of lava flows in which early surface-fed flows tend to be overlain by later tube-fed flows (*62*), and a stratigraphic section comprised of several such sequences consists of units dominated by the different flow types in alternation. Such alternating layers characterize cores obtained in DSDP holes (*63*) and have been observed in the walls of the MAR rift valley (*64*). If the subaerial analogy is correct, the layers should comprise pairs of similar age, the sheet flows being the lower member and pillowed flows the upper member of the pair. Despite much local complexity, with intertonguing of different flow types, the youngest flows tend to be highly channeled pillow lavas overlying sheet flows of similar age (*57*). In a typical cross section of the rift valley, an axial volcano composed of channeled lava flows is built upon a foundation of sheet flows ponded between marginal highs that are the faulted remains of former axial volcanoes (*65*). Volcanism at each locality along the rift is cyclic; variations in sediment cover indicate that the duration of each cycle is on the order of several thousand years. The cycles of volcanism are inferred to correspond to the cycles of magma mixing, and the petrology of the different eruptive phases in the total cycle should reflect the differentiation occurring in the magma chamber and observed in ophiolites.

Dike emplacement at depth is probably a more continuous process in space and time than surface volcanism. The change in stress, $v$, due to the intrusion of a dike is given by

$$v = SEW/L$$

where $S$ is the shape factor of order 1, $E$ is Young's modulus, $W$ is the dike width, and $L$ is the shorter length scale in the plane of the dike. If segments of the ridge crest that are free of recent eruptions did not have dikes at depth, excessive stress would built up in a short period of time. For $W = 1$ m (typical dike width in ophiolites), $E = 0.5$ megabar, $L$ (the thickness of the lid) = 2 km, and at a spreading rate of 6 cm/year a stress of 1 kilobar would be reached in only 70 years ($L$ in this example is the spreading rate multiplied by time). This stress is most likely relieved by dikes that do not reach the surface, leading to surficial volcanism.

Figure 4 also reveals that the active hydrothermal vent fields discovered thus far are located within the narrow zone of most recent volcanism and that they exhibit a cyclic pattern directly associated with the volcanic cycle (*50, 66*). It is possible that magma rising to the surface from ridge-axis magma chambers might move haltingly and be temporarily stored in the dike system, where it could come in contact and interact with hydrothermal fluids circulating through the highly fissured upper crust.

Substantial ambiguity currently exists concerning the degree of fracturing of the oceanic crust and the depth to which the cracking penetrates. Lister (*67*) has argued that water may penetrate to the base of the oceanic crust, and McClain and Lewis (*17*) have pointed out that the subsequent hydration of olivine to ser-

pentine could explain the vast variability reported for the velocities at the base of "layer 3." Nichols *et al.* (*68*) and others have sought to demonstrate that a highly serpentinized lower crust such as that seen in the Point Sal ophiolite (assumed by him to be preemplacement hydration) would form a substantial low-velocity layer at the base of the crust. The resultant structure would act to produce seismic sections that would be classically interpreted as "normal oceanic crust." However, the work of Spudich and Orcutt (*9*) precludes any substantial serpentinization at the base of the crust.

Several investigators have shown that the porosity in the shallow oceanic crust may range from 15 to 20 (*9, 69, 70*). In fact, the EPR 20°N on-bottom gravity data may be interpreted as a 10 percent decrease in crustal density (due to fracturing) rather than as indicative of a shallow magma chamber (*50*). Nevertheless, effective pressure (lithostatic pressure–pore fluid pressure) appears to be effective in raising the in situ velocity to the matrix or uncracked velocity of surface samples within the first 600 m (*66*). Furthermore, the presumption of extensive cracking of the young, upper crust has led Hyndman and Drury (*69*) to predict that the resistivity of the shallow crust would be on the order of 10 ohm-m. Nevertheless, the only active electrical experiment conducted thus far (*50*) provides convincing evidence that the resistivity is ten times larger than this.

## Chemical Constraints on the Hydrothermal Circulation System

The earliest evidence for extensive hydrothermal activity at ridge axes came from the discovery of metal-enriched sediments overlying the young crust on the EPR (*71*). Subsequent exploration has shown these sediments to be commonly associated with intermediate and fast-spreading ridges and to form the basal section in many DSDP cores (*72*).

Subsequent global synthesis of the data for conductive heat flow from the oceanic crust demonstrated unequivocally that there is a major negative thermal anomaly on young crust equivalent to at least half the heat loss required by the thermal models of the plate-forming processes (*64*). This finding indicated that hydrothermal convection could be responsible for the transport of about $5 \times 10^{19}$ calories per year out of the intrusive zone (*73*).

Investigations of the oxygen isotopic systematics of basaltic rocks from the sea floor (*74*) and from ophiolites (*75*) provided independent confirmation of the interaction of seawater with crustal material at high temperatures and to great depths. Measurements of the isotopic composition of "unaltered" primary minerals and of the fractionation between coexisting secondary phases gave estimated temperatures of about 300°C (*76*) and penetration depths of more than 5 km (*77*).

Experimental investigations of basalt-seawater reactions at high temperatures and sea-floor pressures demonstrated that the fluid compositions were profoundly influenced in this process (*78*). If hydrothermal convection is responsible for the anomaly in the conductive heat flow and if the operating temperature of the system is indeed about 300°C, then a volume of water equivalent to the entire ocean must circulate throught he accretion zone approximately every 8 million years. This flow rate is equal to about 0.5 percent of that of the world's rivers (*79*). The experimental data show that the compositional changes imposed on the circulating seawater by reaction with the basalt result in effective transport rates comparable to those of rivers in that anomalies for individual elements are frequently between 100 and 1000 times the average river composition. There is the prospect, therefore, that the composition of seawater is subject to a substantial volcanogenic control.

The first vent fields discovered in the Galápagos Rift at 86°W (*80*) have exiting temperatures less than 20°C above ambient. However, the magnitude and character of the measured chemical anomalies provided clear indications that their temperature of origin was very high, with the exit temperature being an artifact of extensive subsurface entrainment of ambient "ground water" (*81*). Thus the magnesium-to-temperature gradient can be extrapolated to zero concentration near 350°C as can that for sulfate. The solutions are strongly enriched in lithium, potassium, and rubidium, as well as in calcium and barium. The usual sulfide-forming metals are depleted (*82*), an indication that mineralization processes are going on in the crust as the hot acid waters are being neutralized by cold alkaline ground waters. The manganese concentration is also very high.

The anomaly of mantle-derived $^3He$ increases linearly with temperature (*83*). The average $^3He$ flux through the ocean floor is estimated at 4 atoms per square centimeter per second (*77*). If all this is in fact injected at the ridge axis in the same ratio to heat as observed at the Galápagos Rift, then the calculated heat flux is $5 \times 10^{19}$ cal/year, in surprising agreement with the geophysical estimates. This result implies that the Galápagos hot springs have a general compositional significance and allows estimates of the fluxes of the other elements. These fluxes are large and in agreement with what is known about the source and sink terms of the global geochemical mass balance (*81*). Thus the fluxes of magnesium and sulfate into the ridge are equal to the fluvial input and accommodate the hitherto disturbing absence of currently active sedimentary sinks (*82*). The flux of calcium out of the ridge is about equal to that of "new" noncarbonate calcium from the continents: the observed twofold "excess" of calcium in the geologic column over what would be expected from the weathering of average continental igneous rock (*79*) is thus explained. The fluxes of lithium and rubidium are several times those from rivers and determine the observed enrichment of these elements in marine shales over other rock types. Hydrothermal transport of manganese is adequate to account for the entire accumulation of this element in contemporary marine sediments. The total effect of the hydrothermal cycle is to "back-titrate" over half of the bicarbonate fixed in continental weathering of igneous rock (*83*).

These initial speculations based upon the vent fields discovered in the Galápagos Rift were further reinforced by the subsequent discovery in 1979 of much hotter vents on the EPR at 21°N (*50*). In this case, the water exits as clear solutions at 350°C from constructional features of complex mineralogy formed by the precipitation attendant on the mixing of the hydrothermal fluids with the ambient waters. The spectacular black plumes so apparent in the photographs obtained by *Alvin* (*50*) are produced by the same process. The composition of the waters is remarkably consistent with the Galápagos data. The magnesium and sulfate concentrations go to zero within a few degrees of the exit temperature, the $^3He$/heat ratio is identical, and the major element enrichments are within the bounds of the Galápagos extrapolations.

Field measurements of exiting temperatures of 350°C also provided an opportunity to estimate the reaction ratios of seawater to rock. Geothermal waters exchange oxygen isotopes with the rocks and tend to approach an isotopic equilibrium in which the $^{18}O/^{16}O$ ratio of the water undergoes an oxygen shift to higher $^{18}O$ values while the isotopic ratio in the rock is decreased relative to its initial value. In oceanic basalts the principal mineral that can exchange oxygen isotopes with water at moderate tempera-

tures is plagioclase feldspar, and this exchange equilibrium constant has been measured as a function of temperature (*84*). In natural systems such as the ridge-crest basalts, both the water and plagioclase feldspar must be analyzed isotopically, and, since the initial isotopic ratios for seawater and unaltered basalts are known, the equilibrium temperature and the mass ratio of water to rock are then determined. The $^{18}O$ content of vent waters exiting at 21°N plotted against the magnesium concentration show that the extrapolated value at Mg = 0, assumed to characterize the high-temperature fluid end-member, gives an oxygen isotope shift ($\delta^{18}O$) of 1.6 relative to the original seawater (Fig. 5). If we assume a very low ratio of water to rock so that the plagioclase isotopic ratio has not been altered, the temperature corresponding to an isotopic equilibrium difference of 4.3 per mil (rock minus water) is 240°C, which represents a lower limit for the reservoir waters. Such a temperature is clearly not the case, since the fluid emerges at 350°C. If we assume this to be the approximate temperature at which the plagioclase-seawater isotopic equilibrium was achieved, we can then calculate the seawater/plagioclase ratio from the equilibrium difference at 350°C of 1.6 per mil (*84*). The result is a water/plagioclase ratio of 1.7, corresponding to a ratio of water to rock of about unity.

The effect of ridge-crest hydrothermal activity on the major ion chemistry of the ocean and the ultimate composition of the oceanic crust is profound. Pronounced variations in the crustal production rate appear to have occurred in the geologic past (*85*). There should be parallel effects on the relative composition of seawater. There is the possibility of a highly dynamic nonsteady-state balance between (i) the input-determining processes on the continents (primarily orogenic activity), (ii) the spreading rate, which affects both sources and sinks in the new crust, and (iii) oceanic sediment compositions. All are linked through the coupling of spreading rate with mountain building in both continental and, more directly, island-arc environments.

The transport of trace metals sensitive to oxidation-reduction processes is obviously more complex since it is critically dependent on the subsurface "plumbing" (*82*). The admixture of ground water of closely similar composition to the overlying water column moves the mineralization zone from the sea floor, as at 21°N, into the crust itself, as is suspected in the Galápagos Rift. The details of the process should depend critically on the ratio of iron to sulfide in the end-member solutions. If all the seawater sulfide is reduced by ferrous silicates in the hot basalt, then the possibility exists for high ratios (> 2) in systems where the dominant source of the iron is hydrogen metasomatism of silicates. Such solutions on progressive dilution with ground water would evolve toward extreme depletion in sulfide, the oxidation-reduction chemistry being eventually dominated by ferrous iron (*82*). At the other extreme a predominantly pyrite origin for the iron—dissolution of primary igneous sulfides (*86*)—would yield low ratios (< 1) and final solution compositions very low in iron and high in sulfide. The other sulfide-forming cations, copper, nickel, cadmium, and zinc, would mimic iron. There are indications in the Galápagos data that such a progression is taking place (*82*).

It is clear that the degree of subsurface dilution is a major determinant of the final exit composition of the hot springs and hence of their associated chemical precipitates. Low dilution leads to sulfide deposition on the sea floor. Intermediate dilutions lead to iron- or sulfide-dominated systems, depending on the considerations outlined above. Manganese, because of its very slow oxidation kinetics, is unaffected. Hence a very wide range of iron/manganese ratios is to be expected. The vents are too diffuse to dominate the oxidation regime at the sea floor. The oxidized metal-rich sediments will result. At extreme dilutions all reduced species with the exception of manganese will be oxidized below the sea bottom, the hydrogen sulfide to sulfur and eventually sulfate and the ferrous iron to ferric hydroxide. A manganese-dominated system will result, leading to the formation of very pure manganese dioxide crusts unique to the ridge axes.

The duration of venting is also important. The resulting heat loss, for example, from a single 350°C vent is approximately 6 ($\pm$ 2) $\times$ $10^7$ cal per second (*87*). This is equivalent to the expected hydrothermal heat loss for a segment of the spreading ridge 4 to 7 km along strike and out to crust 1 million years old to either side if venting is a steady-state process. It is equivalent to the total theoretical heat loss for a segment 3 to 6 km long (*87*). This result is even more remarkable since there are several vent fields along a 7-km distance containing at least six to ten discrete 350°C vents. Since it is unlikely that a single hydrothermal vent cools such a large segment of the ridge crest, these features must be short-lived. The short duration of venting activity is further supported by the small volume of associated sulfide deposition (*50*), the age and composition of the large clam communities surrounding the hot vents (*66*), and the direct relationship between the hydrothermal activity and the cyclic volcanism (*66*).

For intermediate to fast spreading rates where large axial rifts are not present, the topography at the ridge crest can be used to estimate the long-term hydrothermal flux. Theoretical conductive cooling models predict that the subsidence away from the ridge axis is proportional to the square root of the age of the crust (*88*). The observed topography matches the predicted topography away from the ridge axis. However, topography at the axis deviates from a square-root-of-time dependence. Near the axis, the density difference between the magma chamber and solid crust produces additional elevation. Rapid cooling by hydrothermal circulation would decrease the elevation at the ridge. Approximately 60 m of contraction corresponds to a heat flux of $10^8$ cal/cm$^2$. If the heat anomaly for crust less than 1 million years old, about 7 $\times$ $10^8$ cal/cm$^2$, is due to cooling of the crust by hydrothermal circulation, the effect on the topography should be resolvable. If seismic and gravity data are available to constrain the structure of the magma chamber, then the difference between observed and predicted topography can be used to estimate the average amount of heat removed by hydrothermal circulation.

## Massive Sulfide Deposition

The discovery of the massive sulfide mounds forming at the 350°C vents on the EPR (*50*) is destined to have a profound effect on our understanding of ore-forming processes. For the first time, we have the opportunity to acquire direct information on the composition and temperature of fluids that are forming ore-grade deposits. As these data are combined with analytical data on the hydrothermal precipitates and wall-rock alteration products and considered in the context of the volcanic-tectonic cycle, a general scheme for the evolution of EPR massive sulfide deposits will evolve. Although the chemical systematics remain to be worked out, the EPR discoveries, combined with other pieces of evidence bearing on the environment of metal-rich deposits in modern oceanic crust, allow certain generalizations to be made which shed new light on the genesis of ancient

massive sulfide deposits exposed in ophiolite terrains on the continents.

It is clear that the EPR deposits are not strictly equivalent to ophiolite massive sulfide (OMS) deposits on land, as pointed out by Francheteau *et al.* (*89*) and Edmond *et al.* (*81, 82*). Yet, the many similarities invite comparison. Both types of deposits form on the sea floor in zones of active faulting associated with spreading centers. Sulfide deposition occurs during an early and specific stage of the volcanic cycle. It is known that OMS deposits form during a period of volcanic quiescence and block faulting after the termination of an early stage of pillow-basalt extrusion and within 300 m of the underlying sheeted dike complex and microgabbro (*90, 91*). The EPR deposits appear to form after termination of rapid extension and outpouring of sheet flows and during a period of slow extension and formation of fractured, pillowed axial volcanoes (*65*). The analogies here are fairly striking and suggest that the development of hydrothermal conditions appropriate to the formation of massive sulfides on the sea floor is closely linked to the development of a hot, relatively impermeable volcanic cap, which is not saturated with cold, ambient seawater but which locally is breached by faults capable of focusing the upward flow of heated solutions.

Sulfides are not stable in the low-temperature oxidizing environment of the sea floor at the EPR; the deposits are oxidizing as they form and consist in part of pulverulent iron oxides. The importance of submarine oxidation in the history of OMS deposits was first pointed out by Constantinou and Govett (*92*) in their study of Cyprus. The original deposits, consisting of pyrite with trace amounts of chalcopyrite (0.2 to 0.6 percent copper) and sphalerite (0.08 to 0.2 percent zinc), underwent leaching, before burial, to form an overlying iron oxide gossan (Ochre) and an underlying zone of enriched ore containing secondary sulfides such as covellite, digenite, and bornite. Data on the metal grades of low-grade (primary) and high-grade (secondary) deposits at Cyprus (*93*) suggest that the copper/zinc ratios increase with increasing copper grade, a trend that is compatible with the expected partitioning of copper and zinc during supergene processes. Thus, the high copper/zinc ratios of ores mined at Cyprus probably are not representative of the primary deposits, which would have displayed ratios closer to unity and hence closer to those determined so far from EPR samples. That the EPR samples represent primary ratios remains to be demonstrated, but it is doubtful that a supergene enrichment process is possible because the highly porous nature of these deposits would inhibit development of the low oxidation states required. Rather, copper and zinc are released to seawater during the formation of iron oxides and native sulfur.

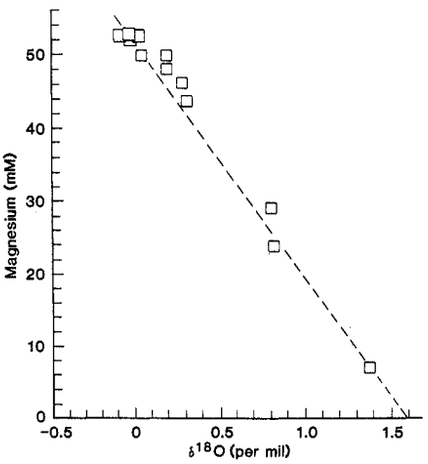


Fig. 5. Magnesium concentration and $^{18}O$ of water samples at the EPR (21°N). The line is fitted by eye and gives a $\delta^{18}O$ value of +1.6 per mil for the 350°C hydrothermal fluid.

In addition to the analogies discussed above, there exist fundamental differences that are perhaps more important in understanding the processes that lead to the formation of large and economically attractive metalliferous deposits; these differences relate to both metal grade and scale. Individual EPR deposits contain a few tons of sulfide (although the volume of sulfides in the underlying fissure complex is not known), and the majority probably are oxidized and destroyed before they are transported off-axis. In contrast, the OMS deposits contain a few hundred thousand to a few million tons of sulfide; their thickness, combined with burial by younger flows, ensured their preservation.

The composition and temperature of hydrothermal fluids of seawater origin approaching the sea floor on the last leg of their convective trip may largely be a function of spreading rate. Relatively slow spreading rates are characterized by relatively intense tectonic activity, increased permeability of ridge-crest areas, and hence extensive seawater circulation and low exit temperatures. Also, high ratios of crystal to glass in the basalts would lower reactivities. The result would be low-temperature hydrothermal springs containing low iron/manganese ratios and low amounts of sulfur. In contrast, relatively fast spreading rates are characterized by less intense tectonic activity and shallow magma chambers, resulting in less extensive seawater circulation and higher exit temperatures. In addition, lower ratios of crystal to glass would enhance the extent of reaction between seawater and basalt. The result would be high-temperature springs with high iron/manganese ratios and high concentrations of sulfur.

The correlation of metal-rich OMS deposits with fast spreading rates is an important hypothesis. All the OMS deposits are Phanerozoic in age, but such deposits do not occur exclusively in ophiolite terrains. They first appear in Ordovician rocks in Newfoundland (*94*), reach a peak in the Mesozoic ophiolites of Cyprus (*90*), Turkey (*91*), and the North American cordillera (*95*), and in the Tertiary ophiolites of Turkey (*96*) and the Philippines (*97*). Do these age groups represent periods of fast spreading, and, if so, what can one expect to find at 15°S on the EPR where the opening rate is 17 cm/year?

## Conclusions

This article is an initial attempt to integrate several separate lines of evidence presently being developed to define the complex structure and dynamic processes associated with the magma chamber system underlying the MOR. It is far from perfect. The varied approaches and the terminology of the disciplines represented by the authors makes rigorous comparisons difficult. Some of the authors draw their conclusions from ancient ophiolite complexes on land of unknown spreading rates and other conclusions are heavily based upon drilling efforts in slow-spreading segments of the MOR, while the geophysical observations come largely from moderate- to fast-spreading segments of the EPR. Owing to the sparsity of comparable data sets collected in spreading segments of the MOR having similar rates of accretion, a gross generalization was made in the preparation of this article that a single model of the underlying magma chamber could be constructed. This assumption probably will prove to be unfounded, particularly for slow-spreading segments. We do, however, believe that the writing of this article has provided a valuable service to those who participated in its preparation, as it exposed each of us to several lines of inquiry we understood poorly. Perhaps the reader will share a similar experience and overlook our sudden changes in vocabularies, as

those working in these diverse disciplines attempt to define a common understanding of a complex system important to all of us.

### References and Notes


1. M. F. Maury, *Physical Geography of the Sea* (Harper, New York, 1871).
2. L. M. Dorman and B. T. R. Lewis, *J. Geophys. Res.* **75**, 3357 (1970); *ibid.* **77**, 3068 (1972); B. T. R. Lewis and L. M. Dorman, *ibid.* **75**, 3367 (1970).
3. J. R. Cochran, *ibid.* **84**, 4713 (1979).
4. N. H. Sleep, *ibid.* **80**, 4037 (1975).
5. R. L. Parker and D. W. Oldenburg, *Nature (London)* **242**, 122 (1973); N. H. Sleep, *Geol. Soc. Am. Bull.* **85**, 1225 (1974); D. W. Oldenburg, *Geophys. J. R. Astron. Soc.* **43**, 425 (1975).
6. J. A. Orcutt, B. Kennett, L. R. Dorman, W. Prothero, *Nature (London)* **256**, 475 (1975).
7. J. A. Orcutt, B. L. N. Kennett, L. R. Dorman, *Geophys. J. R. Astron. Soc.* **45**, 305 (1976).
8. B. R. Rosendahl, R. W. Raitt, L. R. Dorman, L. D. Bibee, D. M. Hussong, G. H. Sutton, *J. Geophys. Res.* **81**, 5294 (1976).
9. P. K. P. Spudich and J. A. Orcutt, *ibid.* **85**, 1409 (1980).
10. P. K. P. Spudich, M. H. Salisbury, J. A. Orcutt, *Geophys. Res. Lett.* **5**, 341 (1978).
11. M. Ewing, A. P. Crary, H. M. Rutherford, *Geol. Soc. Am. Bull.* **48**, 753 (1937).
12. B. L. N. Kennett and J. A. Orcutt, *J. Geophys. Res.* **81**, 4061 (1976).
13. D. V. Helmberger, *Bull. Seismol. Soc. Am.* **58**, 179 (1968).
14. B. L. N. Kennett, *Geophys. J. R. Astron. Soc.* **42**, 579 (1975).
15. I. Reid, J. A. Orcutt, W. A. Prothero, *Geol. Soc. Am. Bull.* **88**, 678 (1977).
16. T. J. Herron, W. J. Ludwig, P. L. Stoffa, T. K. Kan, P. Buhl, *J. Geophys. Res.* **83**, 798 (1978).
17. J. S. McClain and B. T. R. Lewis, *Mar. Geol.*, in press.
18. B. R. Rosendahl, S. D. Russell, L. M. Dorman, S. Johnson, *Eos Trans. Am. Geophys. Union* **59**, 1139 (1978).
19. J. Bibee, thesis, Scripps Institution of Oceanography (1979).
20. S. Russell, thesis, Duke University (1979).
21. J. Mueller, thesis, Duke University (1979).
22. W. Scarlett, thesis, Duke University (1979).
23. E. M. Moores and F. J. Vine, *Philos. Trans. R. Soc. London Ser. A* **268**, 443 (1971); N. I. Christensen, N. I. Salisbury, M. H. Salisbury, *Rev. Geophys. Space Phys.* **13**, 57 (1975); N. I. Christensen and J. D. Smewing, *J. Geophys. Res.*, in press.
24. C. A. Hopson *et al.*, *J. Geophys. Res.*, in press.
25. J. M. Rhodes, M. A. Dungan, D. P. Blanchard, P. E. Long, *Tectonophysics* **55**, 35 (1979); D. Walker, T. Shibata, S. E. DeLong, *Contrib. Mineral. Petrol.* **70**, 111 (1979).
26. W. B. Bryan and J. G. Moore, *Geol. Soc. Am. Bull.* **88**, 556 (1977).
27. R. Hekinian, J. G. Moore, W. B. Bryan, *Contrib. Mineral. Petrol.* **58**, 83 (1976); D. Stakes, J. W. Shervais, C. A. Hopson, *Geol. Soc. Am. Abstr. Programs*, in press.
28. G. R. Byerly and T. L. Wright, *J. Volcanol. Geothermal Res.* **3**, 229 (1978).
29. N. S. MacLeod, *U.S. Geol. Surv. Bull.*, in press.
30. J. F. Dewey and W. S. F. Kidd, *Geol. Soc. Am. Bull.* **88**, 960 (1977).
31. M. H. Salisbury, thesis, University of Washington (1974); N. I. Christensen, *Tectonophysics* **47**, 131 (1978).
32. C. A. Hopson and J. S. Pallister, in *Proceedings of the International Ophiolite Symposium*, P. Aanayiotou, Ed. (Cyprus Geological Survey, Nicosia, 1980).
33. D. Greenbaum, *Nature (London) Phys. Sci.* **238**, 18 (1972).
34. E. D. Jackson, H. W. Green II, E. M. Moores, *Geol. Soc. Am. Bull.* **86**, 390 (1975).
35. C. A. Hopson and C. J. Frano, *Oreg. Dep. Geol. Miner. Ind. Bull.* **95**, 161 (1977); J. D. Smewing, in *Tethyan Ophiolites* (Akademiya Nauk Ministerstvo Geologii, Moscow, 1981).
36. J. S. Pallister and C. A. Hopson, *J. Geophys. Res.*, in press.
37. J. R. Cann, *Geophys. J. R. Astron. Soc.* **39**, 169 (1974); B. R. Rosendahl, *J. Geophys. Res.* **81**, 5305 (1976).
38. H. L. Davies, *Aust. Bur. Miner. Resour. Geol. Geophys. Bull.* **128** (1971).
39. R. G. Coleman, *Ophiolites* (Springer, New York, 1977); ——— and Z. E. Peterman, *J. Geophys. Res.* **80**, 1099 (1975).
40. C. A. Hopson, J. N. Mattinson, E. A. Pessagno, in *Geotectonic Development of California*, W. G. Ernst, Ed. (Prentice-Hall, Englewood Cliffs, N.J., in press).
41. J. M. Hall and P. T. Robinson, *Science* **204**, 573 (1979).
42. E. G. Nisbet and C. M. R. Fowler, *Geophys. J. R. Astron. Soc.* **54**, 631 (1978).
43. R. C. Lilwall, T. J. G. Francis, I. T. Porter, *ibid.* **55**, 255 (1978).
44. T. N. Irvine, *Carnegie Inst. Washington Yearb.* **76**, 454 (1977); F. Baudier and R. G. Coleman, *J. Geophys. Res.*, in press.
45. D. C. Presnall, J. R. Dixon, T. H. O'Donnell, S. A. Dixon, *J. Petrol.* **20**, 3 (1979).
46. J. D. Smewing, *J. Geophys. Res.*, in press.
47. F. A. Frey, W. B. Bryan, G. Thompson, *ibid.* **79**, 5507 (1974).
48. W. G. Melson, P. L. Vallier, P. L. Wright, G. Byerly, J. Nelen, *Geophys. Monogr. Am. Geophys. Union* **19**, 351 (1976).
49. W. B. Bryan, G. Thompson, F. A. Frey, J. S. Dickey, *J. Geophys. Res.* **81**, 4285 (1976).
50. RISE Project Group, *Science* **207**, 1421 (1980).
51. D. P. Blanchard, J. M. Rhodes, M. A. Dungan, K. V. Rogers, C. H. Donaldson, J. C. Brannon, J. W. Jacobs, E. K. Gibson, *J. Geophys. Res.* **81**, 4231 (1976).
52. C. H. Langmuir, J. F. Bender, A. E. Bence, G. N. Hanson, S. R. Taylor, *Earth Planet. Sci. Lett.* **36**, 133 (1977); W. M. White, *Carnegie Inst. Washington Yearb.* **78**, 325 (1979).
53. K. C. Macdonald, *Geol. Soc. Am. Bull.* **88**, 541 (1977).
54. K. Klitgord, *Geophys. J. R. Astron. Soc.* **43**, 387 (1975).
55. K. C. Macdonald, S. P. Miller, S. P. Huestis, F. N. Spiess, *J. Geophys. Res.* **85**, 3670 (1980).
56. K. C. Macdonald, S. P. Miller, L. Shure, B. P. Luyendyk, T. Atwater, *Eos Trans. Am. Geophys. Union* **60**, 813 (1979).
57. R. D. Ballard, R. T. Holcomb, Tj. H. van Andel, *J. Geophys. Res.* **84**, 5407 (1979).
58. R. T. Holcomb, Tj. H. van Andel, R. D. Ballard, *Eos Trans. Am. Geophys. Union* **60**, 970 (1979).
59. H. Schouten and C. Denham, *Am. Geophys. Union Maurice Ewing Ser.* **2**, 151 (1979).
60. R. D. Ballard and J. G. Moore, *Photographic Atlas of the Mid-Atlantic Ridge* (Springer, New York, 1977).
61. P. A. Swanson, *Geol. Soc. Am. Bull.* **84**, 615 (1973).
62. R. T. Holcomb, *U.S. Geol. Surv. Map MF-811* (1976).
63. W. B. Bryan *et al.*, *Geotimes* **22**, 22 (1977).
64. R. D. Ballard, T. Atwater, D. Stakes, K. Crane, C. Hopson, *Eos Trans. Am. Geophys. Union* **59**, 1198 (1978).
65. Tj. H. van Andel and R. D. Ballard, *J. Geophys. Res.* **84**, 5390 (1979).
66. K. Crane and R. D. Ballard, *ibid.*, in press.
67. C. R. B. Lister, *Geophys. J. R. Astron. Soc.* **39**, 465 (1974); *Tectonophysics* **37**, 203 (1977).
68. J. Nichols, N. Warren, B. P. Luyendyk, P. Spudich, *Geophys. J. R. Astron. Soc.*, in press.
69. R. D. Hyndman and M. J. Drury, *J. Geophys. Res.* **81**, 4042 (1976).
70. R. D. Whitmarsh, *Earth Planet. Sci. Lett.* **37**, 451 (1978); T. J. G. Francis, *J. Geophys. Res.* **81**, 4361 (1976); R. J. Kirkpatrick, *ibid.* **84**, 178 (1979).
71. K. Bostrom and M. N. A. Peterson, *Econ. Geol.* **61**, 1258 (1965).
72. G. R. Heath and J. Dymond, *Geol. Soc. Am. Bull.* **88**, 723 (1977).
73. T. J. Wolery and N. H. Sleep, *J. Geol.* **84**, 249 (1976).
74. K. Muehlenbachs and R. N. Clayton, *Can. J. Earth Sci.* **9**, 172 (1972).
75. M. Magaritz and H. P. Taylor, Jr., *Earth Planet. Sci. Lett.* **23**, 8 (1974).
76. K. Muehlenbachs and R. N. Clayton, *Can. J. Earth Sci.* **9**, 471 (1972).
77. R. T. Gregory and H. P. Taylor, Jr., *Earth Planet. Sci. Lett.*, in press.
78. M. J. Mottl and H. D. Holland, *Geochim. Cosmochim. Acta* **42**, 1103 (1978).
79. R. M. Garrels and F. T. Mackenzie, *The Evolution of Sedimentary Rocks* (Norton, New York, 1971), p. 397.
80. J. B. Corliss *et al.*, *Science* **203**, 1073 (1979).
81. J. M. Edmond, C. Measures, R. E. McDuff, L. H. Chan, R. Collier, B. Grant, L. I. Gordon, J. B. Corliss, *Earth Planet. Sci. Lett.* **46**, 1 (1979).
82. J. M. Edmond, C. Measures, B. Mangum, B. Grant, F. R. Sclater, R. Collier, A. Hudson, L. I. Gordon, J. B. Corliss, *ibid.*, p. 19.
83. W. J. Jenkins, J. M. Edmond, J. B. Corliss, *Nature (London)* **272**, 156 (1978).
84. J. R. O'Neil and H. P. Taylor, *Am. Mineral.* **52**, 1414 (1967).
85. D. L. Turcotte and K. Burke, *Earth Planet. Sci. Lett.* **41**, 341 (1979).
86. M. J. Mottl and H. D. Holland, *Geochim. Cosmochim. Acta* **43**, 869 (1979).
87. K. C. Macdonald, K. Becker, F. N. Spiess, R. D. Ballard, *Earth Planet. Sci. Lett.* **48**, 1 (1980).
88. A. M. Trehu, *ibid.* **27**, 287 (1975); B. Parsons and J. G. Sclater, *J. Geophys. Res.* **82**, 803 (1977).
89. J. Francheteau *et al.*, *Nature (London)* **277**, 523 (1979).
90. D. L. Searle, *Trans. Am. Inst. Min. Metall. Pet. Eng.* **81**, 189 (1977).
91. R. W. Hutchinson, *Econ. Geol.* **68**, 1223 (1973).
92. G. Constantinou and G. J. S. Govett, *Trans. Am. Inst. Min. Metall. Pet. Eng.* **81**, 34 (1972).
93. R. A. M. Wilson and F. T. Ingham, *Cyprus Geol. Surv. Dep. Mem. 1* (1959); L. M. Bear, *Miner. Resour. Min. Ind. Cyprus Bull. Geol. Surv. Cyprus 1* (1963).
94. H. R. Peters, *Geol. Assoc. Can. Spec. Pap. 4* (1967), p. 171; H. D. Upadhyay and D. F. Strong, *Econ. Geol.* **68**, 161 (1973).
95. M. C. Stinson, *Calif. J. Mines Geol.* **53**, 9 (1957).
96. W. R. Griffitts, J. P. Albers, O. Oner, *Econ. Geol.* **67**, 701 (1972).
97. L. Bryner, *Philipp. Bur. Mines Rep. Invest. No. 60* (1967).
98. R. D. Ballard, Tj. H. van Andel, R. T. Holcomb, *J. Geophys. Res.*, in press.


99. We thank C. Drake for encouraging us to attempt such an undertaking. We also thank the Office of Naval Research and the National Science Foundation for their loyal support of the research programs, which have provided us with the diverse data base presented here. The final preparation of this manuscript was funded through a grant (N00014-79-C-0071) to the Woods Hole Oceanographic Institution by the Office of Naval Research. Woods Hole Oceanographic Institution Contribution No. 4787.